RESEARCH ARTICLE

WILEY

Mechanical properties of 3D-printed and milled composite resins for definitive restorations: An in vitro comparison of initial strength and fatigue behavior

Elisabeth Prause DMD [1] | Tine Malgaj DMD, PhD [2] | Andraž Kocjan MCheE, PhD [3] |
Florian Beuer DMD, PhD [1] | Jeremias Hey DMD, PhD [4] |
Peter Jevnikar DMD, PhD [2] | Franziska Schmidt Dr. Ing., PhD [1]

[1]Department of Prosthodontics, Geriatric Dentistry and Craniomandibular Disorders, Charité-Universitätsmedizin Berlin, Berlin, Germany

[2]Department of Prosthodontics, Faculty of Medicine, University of Ljubljana, Ljubljana, Slovenia

[3]Department for Nanostructured Materials, Jožef Stefan Institute, Ljubljana, Slovenia

[4]Department of Prosthodontics, School of Dental Medicine, Martin-Luther-University, Halle, Germany

Correspondence
Peter Jevnikar, Department of Prosthodontics, Faculty of Medicine, University of Ljubljana, Hrvatski trg 6, SI-1000 Ljubljana, Slovenia.
Email: peter.jevnikar@mf.uni-lj.si

Abstract

Objective: To evaluate the flexural strength and fatigue behavior of a novel 3D-printed composite resin for definitive restorations.

Materials and Methods: Fifty disc-shaped specimens were manufactured from each of a nanohybrid composite resin (NHC), polymer-infiltrated ceramic network (PICN), and 3D-printed composite resin (3D) with CAD-CAM technology. Biaxial flexural strength (σ_{in}) ($n = 30$ per group) and biaxial flexural fatigue strength (σ_{ff}) ($n = 20$ per group) were measured using piston-on-three-balls method, employing a staircase approach of 10^5 cycles. Weibull statistics, relative-strength degradation calculations, and fractography were performed. The results were analyzed with 1-way ANOVA and Games-Howell post hoc test ($\alpha = 0.05$).

Results: Significant differences in σ_{in} and σ_{ff} among the groups ($p < 0.001$) were detected. The NHC group provided the highest mean ± standard deviation σ_{in} and σ_{ff} (237.3 ± 31.6 MPa and 141.3 ± 3.8 MPa), followed by the PICN (140.3 ± 12.9 MPa and 73.5 ± 9.9 MPa) and the 3D (83.6 ± 18.5 MPa and 37.4 ± 23.8 MPa) groups. The 3D group exhibited significantly lower Weibull modulus ($m = 4.7$) and up to 15% higher relative strength degradation with areas of nonhomogeneous microstructure as possible fracture origins.

Conclusions: The 3D-printed composite resin exhibited the lowest mechanical properties, where areas of nonhomogeneous microstructure developed during the mixing procedure served as potential fracture origins.

Clinical Significance: The clinical indications of the investigated novel 3D-printed composite resin should be limited to long-term provisional restorations. A cautious procedure for mixing the components is crucial before the 3D-printing process, since nonhomogeneous areas developed during the mixing could act as fracture origins.

1 | INTRODUCTION

Dental composite resins, in combination with innovative computer-aided design/computer-aided manufacturing (CAD/CAM) and adhesive technologies, have been widely used as an alternative restorative material in contemporary, minimally invasive prosthodontics.[1,2] The main advantages of composite resins over glass–ceramics include the low abrasiveness with respect to antagonist teeth,[3] a better absorption of the functional stresses,[4] and favorable handling properties, including intra-oral repairability.[1] In addition, adequate mechanical properties for ultra-thin bonded composite resin restorations have been reported in vitro.[5] Clinical trials have further confirmed the promising performance of such composite restorations,[1,2] suggesting their potential for use as a material that can address the biomimetic principles of tissue preservation.[6]

In the past decade, indirect composite resin restorations were fabricated with a CAD/CAM workflow using subtractive methods such as milling.[7] In this procedure, a lot of material is discarded compared to the amount needed for the final restoration. In addition, the milling process is time-consuming, while its accuracy depends on the geometry of the milling bur. In light of these concerns, three-dimensional (3D) printing as an additive-manufacturing method for dental composite restorations was recently proposed.[8] This approach offers a reduced consumption of material, while multiple and complex restoration geometries can be produced simultaneously, reducing both the manufacturing time and the costs.[9,10]

To achieve adequate 3D-printing outcomes, a more flowable pre-polymerized composite resin that has a reduced amount of inorganic filler is needed. However, the absence or a decreased amount of inorganic filler lowers the mechanical properties of 3D-printed resin or composite resin, narrowing their clinical indications to long-term interim restorations.[11] Recently, novel 3D-printed composite resins with ceramic fillers have been marketed as materials for single-tooth definitive restorations. Nevertheless, before these materials can be clinically recommended, more independent preclinical and clinical data about their long-term mechanical behavior[9] are needed.

Current in vitro studies on 3D-printed resins and composite resins are mainly limited to static tests evaluating the intrinsic material properties such as the material strength,[11–20] resilience,[17] fracture toughness,[17,20] microhardness,[12,15,21,22] wear,[23] surface roughness,[19,22,24] and the modulus of elasticity.[12,15,18,22] However, these tests do not relate to clinically relevant failure mechanisms such as fatigue, which involves the growth of subcritical defects during cyclic loading in a humid environment.[25] Further, although 3D printing could introduce subcritical defects that can serve as potential fracture origins, only a few studies have conducted a fractographic analysis subsequent to the strength testing,[14,16,18] and none after the fatigue testing.[20,26–28] Therefore, the nature of the flaw population and the fracture patterns in 3D-printed composite resins should be comprehensively investigated using detailed fractography complementing the fatigue testing.

Fatigue strength has been shown to closely correlate with the clinical outcomes of composite resin restorations, offering a rough prediction of their clinical performance.[29,30] Since there is no data confirming the clinical indications of novel 3D-printed composite resins proposed for definitive restorations, it would be sensible to compare their mechanical properties, particularly their fatigue behavior, with those of clinically approved milled composite resins.

A variety of composite resins with different microstructures, often determining their specific clinical applications, have been introduced and investigated. For example, nanohybrid composite (NHC) resins, with a larger content of filler particles, have been extensively investigated, showing promising mechanical properties, especially a high fatigue flexural strength.[29,31] In addition, polymer-infiltrated ceramic network (PICN) materials are gaining interest from clinicians because of their unique microstructure, which provides a favorable elastic modulus and flexural load energy, making them an alternative in high-occlusal-load scenarios.[32] Both PICN and NHC materials have shown promising clinical results in various indications such as inlays,[33] onlays,[34] crowns,[2,35] and ultra-thin occlusal veneers,[1,36] making them an ideal reference for relating fatigue behavior to novel 3D-printed composite resins and estimating their clinical performance.

Therefore, the present study aimed to evaluate the initial and fatigue biaxial flexural strength of a novel 3D-printed composite resin intended for definitive restorations and relate it to clinically validated milled NHC and PICN composite resins. Furthermore, the relative strength degradation was assessed to compare the fatigue susceptibility of the tested materials, and fractography was used to assess the fracture pattern and fracture origins of the materials. The following research hypotheses were investigated: (1) there were differences in the mechanical properties (initial and fatigue biaxial flexural strengths) among the evaluated resin composites; (2) there were differences in the fracture patterns of the evaluated composite resins, influenced by the manufacturing method.

2 | MATERIALS AND METHODS

2.1 | Specimen preparation

Disc-shaped specimens with a diameter of 15 mm and a height of 1.5 mm were designed using computer-aided design (CAD) software (FreeCAD 0.20, FPA). The specimen's geometry was prepared in accordance with the previously established experimental settings[37] based on the international standard ISO 6872.[38] The specimens were divided into three groups ($n = 50$) according to the material used (Table 1): milled from a nanohybrid composite resin (group NHC) (Grandio, VOCO, Cuxhaven, Germany), milled from a polymer-infiltrated ceramic

TABLE 1 Study materials.

Group	Material	Lot. number	Commercial name	Composition
3D	3D-printed composite resin	600317	VarseoSmile Crown plus	30–50 wt% inorganic fillers (particle size 0.7 μm) silanized dental glass, methyl benzoylfor-mate, diphenyl (2,4,6-trimethylbenzoyl) phosphine oxide
PICN	Polymer-infiltrated ceramic network	56560	Vita Enamic	UDMA, TEGDMA (14 wt%) feldspar ceramic network (86 wt%)
NHC	Nanohybrid composite resin	1711521	Voco Grandio	86 wt% inorganic fillers, UDMA, DMA (14 wt%)

Abbreviations: DMA, dimethyl methacrylate; TEGDMA, triethylene glycol dimethacrylate; UDMA, urethane dimethacrylate.

network (group PICN) (Enamic, Vita Zahnfabrik, Bad Sackingen, Germany), and printed from composite resin (group 3D) (VarseoSmile Crown Plus, Bego, Bremen, Germany). The specimens in the NHC and PICN groups were milled in a 5-axis computer numerical control (CNC) milling machine (K5, vhf camfacture, Ammerbuch, Germany) under dry conditions with a diamond tool.

The specimens in the 3D-printed group were produced by digital light processing (DLP) in a 3D printer (Varseo XS, Bego, Bremen, Germany). The discs were positioned vertically on the build platform at a distance of 2 mm above the platform using nesting software (CAMcreator; Bego, Bremen, Germany). The discs were printed with a printing-layer thickness of 50 μm. After removing them from the build platform, the specimens were ultrasonically cleaned in 99% isopropanol, first for 3 min of rough cleaning, followed by 2 min of final cleaning, and then dried in an oil-free airflow. After removing the support structures, glass bead blasting (Perlablast micro, Bego, Bremen, Germany) under a pressure of 1.5 bar was performed to remove a white layer of unattached filler particles. The specimens were polymerized in a curing device (Otoflash, Bego, Bremen, Germany) for 2 × 1500 flashes. None of the specimens were polished before testing.

The dimensions of each specimen were measured with a digital caliper having an accuracy of 0.01 mm. The disc diameter was measured at two points by rotating the specimen by 90°. The thickness was assessed at three separate points, each positioned 120° apart along a 5-mm-diameter circumference originating from the center of the disc. The final milled specimens exhibited a mean thickness of 1.49 ± 0.02 mm, while the 3D group exhibited a thickness of 1.48 ± 0.03 mm. The specimens were not polished since the flaws introduced during the milling and printing procedure and their effect on the critical defect distribution were the study's main interest. The specimens were stored in distilled water at 37°C for 14 days before the mechanical testing.

2.2 | Initial biaxial flexural strength

The initial biaxial flexural strength (σ_{in}) was measured using the piston-on-three-balls method (P3B) according to the international standard ISO 6872.[38] Thirty disc specimens per group were positioned on three steel balls of 1 mm diameter, 120° apart on an 11-mm-diameter circumference. The load was applied at the center of the specimen through a flat piston in a hydraulic testing machine

(Instron 8871, Instron, Norwood, USA). After fracture, the fragments were carefully collected and assembled. The initial biaxial flexural strength (σ_{in}) was calculated using the following equations[38]:

$$\sigma_{in} = \frac{-0.2387P(X-Y)}{h^2} \quad (1)$$

$$X = (1+\nu)\ln\left(\frac{r_2}{r_3}\right)^2 + \left[\frac{1-\nu}{2}\right]\left(\frac{r_2}{r_3}\right)^2 \quad (2)$$

$$Y = (1+\nu)\left[1+\ln\left(\frac{r_1}{r_3}\right)^2\right] + (1-\nu)\left(\frac{r_1}{r_3}\right)^2 \quad (3)$$

where P is the failure load (in N); h is the specimen height at fracture origin; ν is the Poison's ratio ($\nu = 0.30$); r_1 is the circle radius of the steel balls (5.5 mm); r_2 is the radius of the loaded area (1.0 mm); r_3 is the specimen radius. A Poisson's ratio of 0.3 was used for all three materials.[39,40]

2.3 | Biaxial flexural fatigue strength

The biaxial flexural fatigue strength (σ_{ff}) or the residual fracture strength was measured using the piston-on three-balls (P3B) method with the same experimental set-up as for measuring the initial biaxial flexural strength. Following the established testing protocol,[31,41,42] 20 specimens per group were cyclically loaded in the same hydraulic testing machine (Instron 8871, Instron, Norwood, USA). The tests were conducted for 10^5 cycles at a frequency of 10 Hz in distilled water at 37°C, using the staircase approach.[43,44] The maximum stress for the first specimen was empirically set to 50% of the measured initial strength (σ_{in}) and was increased or decreased by an increment of 5% of the initial strength (σ_{in}) for each successive specimen.[45] If the previous specimen failed, the maximum applied stress was decreased and vice-versa.

2.4 | Fractography

Representative specimens from statically and cyclically loaded groups were investigated under a scanning electron microscope (SEM) (JSM-7600F, Jeol, Tokyo, Japan) to identify the fracture pattern,

location, and size of the critical defects causing failure. Before the SEM investigation, selected fracture surfaces were carbon coated using a carbon filament on a Sputter Coater (SCD 050, Bal-tec, Balzers, Liechtenstein). The representative specimen was determined from the σ_{in} and σ_{ff} values closest to the mean value for each group.

2.5 | Statistical analysis

The sample size of 30 specimens for the Weibull analysis was set according to ISO 6872.[38] The biaxial flexural strength data obtained with the P3B test were analyzed using Weibull statistics according to the European standard EN 843-5.[46] The Weibull modulus (m) and the characteristic strength (σ_0) were derived from a double logarithmic plot using a maximum likelihood estimation to fit the data. The characteristic strength (σ_0) is the stress at a failure probability of ~63.2%, while the Weibull modulus (m) is the slope of the regression and is a measure of the underlying distribution of critical defects at the surface or in the volume of the material, reflecting the material's reliability. The characteristic strength (σ_0), Weibull modulus (m), and their confidence intervals were corrected using specific weighting factors taking into account the number of tested specimens ($n = 30$) according to EN 843-5.[46]

The biaxial flexural fatigue strength (σ_{ff}) and its standard deviation were calculated using Equations (4) and (5)[43,44]:

$$\sigma_{ff} = X_0 + d\left(\frac{\sum i n_i}{\sum n_i} \pm 0.5\right) \quad (4)$$

$$SD = 1.62 d\left(\frac{\sum n_i \sum i^2 n_i - (\sum i n_i)^2}{\left(\sum n_i\right)^2} + 0.029\right) \quad (5)$$

A biaxial flexural fatigue strength analysis is based on the least frequent event, where only failures or non-failures are used in the calculation. In Equation (4), the minus sign is used when the calculation is based on the non-failures. The lowest stress level is denoted as $i = 0$, the next as $i = 1$, etc. n_i is the number of failed or non-failed specimens at a given stress level. Since the data are concentrated around the mean stress value, 20 specimens per group are sufficient for this method.[43] The differences in the fatigue susceptibility among different materials were assumed by comparing relative strength degradations (($\sigma_{in} - \sigma_{ff})/\sigma_{in}$).[31,41]

The statistical analysis was performed using statistical software (IBM SPSS Statistics, v27.0, IBM, New York, USA). Shapiro–Wilk and

Levene tests were performed to assess the assumptions of the normality of the data and the homogeneity of variances. A 1-way analysis of variance with the Welch statistic and Games-Howell post hoc test were carried out to assess the differences in the initial biaxial flexural strength (σ_{in}) and the biaxial flexural fatigue strength (σ_{ff}) among the groups ($\alpha = 0.05$). The characteristic strength (σ_0) and Weibull modulus (m) among the groups were compared by observing the overlap of the corresponding 95% confidence intervals.

3 | RESULTS

3.1 | Initial biaxial flexural strength

Means and standard deviations of the initial biaxial flexural strength (σ_{in}), the biaxial flexural fatigue strength (σ_{ff}), the strength degradation ($\sigma_{in} - \sigma_{ff}$), and the relative strength degradation (in %) are presented in Table 2. The Weibull distribution parameters for the specimens tested in P3B are summarized in Table 3.

Statistically significant differences in the initial biaxial flexural strength (σ_{in}) among the groups were found ($p < 0.001$), where the NHC group had the highest (237.3 MPa), and the 3D group the lowest, mean value (83.5 MPa). The probability of failure versus the failure stress of the different specimens in a Weibull diagram is presented in Figure 1. Accordingly, the NHC group exhibited the highest ($\sigma_0 = 250.0$ MPa), whereas the 3D group had the lowest characteristic strength ($\sigma_0 = 90.9$ MPa). Furthermore, 95% confidence intervals for the characteristic strengths did not overlap for all the groups, indicating relevant differences among the groups (Table 3). The Weibull moduli for the NHC and PICN groups were comparable, with their 95% confidence intervals not overlapping with the 3D group, indicating a significantly lower Weibull modulus for the 3D group.

3.2 | Biaxial flexural fatigue strength

The staircase method provided significantly different biaxial flexural fatigue strength (σ_{ff}) values calculated for the experimental groups ($p < 0.001$), where the NHC group exhibited the highest (141.3 MPa) and the 3D group the lowest (37.4 MPa) values (Table 2). Figure 2 shows the data points of the staircase fatigue test for all the experimental groups. The 3D group exhibited a significantly higher strength

Group	σ_{in} (MPa)	σ_{ff} (MPa)	$\sigma_{in} - \sigma_{ff}$ (MPa)	Strength degradation (%)
3D	83.5 ± 18.5[a]	37.4 ± 23.8[a]	46.2	55.2
PICN	140.3 ± 12.9[b]	73.5 ± 9.9[b]	66.8	48.6
NHC	237.3 ± 31.6[c]	141.3 ± 3.8[c]	96.0	40.5

TABLE 2 Means ± standard deviations of initial biaxial flexural strength (σ_{in}) and biaxial flexural fatigue strength (σ_{ff}), strength degradation ($\sigma_{in} - \sigma_{ff}$), and relative strength degradation.

Note: The same lower-case letters denote no statistical differences among groups ($p > 0.05$).
Abbreviations: NHC, nanohybrid composite resin; PICN, polymer-infiltrated ceramic network; 3D, 3D-printed composite resin.

TABLE 3 Results of Weibull analysis.

Group	σ_0 (MPa)		m	
3D	90.9	(86.4–95.5)	4.7	(3.3–6.0)
PICN	145.7	(138.5–153.1)	13.0	(9.1–16.7)
NHC	250.0	(241.2–260.8)	8.6	(6.0–11.1)

Note: Characteristic strength (σ_0) and Weibull modulus (m) with the 95% confidence intervals (in parentheses).
Abbreviations: NHC, nanohybrid composite resin; PICN, polymer-infiltrated ceramic network; 3D, 3D-printed composite resin.
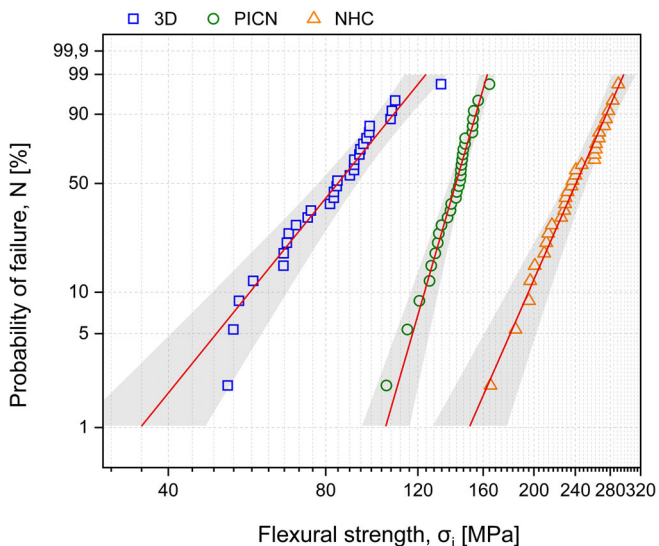

FIGURE 1 Probability of failure (*P*) versus failure stress (σ) for experimental groups. NHC, nanohybrid composite resin; PICN, polymer-infiltrated ceramic network; 3D, 3D-printed composite resin.

degradation of 55.2%, while the NHC group exhibited the lowest strength degradation of 40.5% (Table 2).

3.3 | Fractography

Fractographic analysis was performed following an Academy of Dental Materials guidance document.[47] Common fractographic features, such as compression curls, hackle lines, and fracture origin, were observed. The compression curls are opposite to the surface that is subjected to the tensile stress. Hackle lines indicate the origin and direction of the crack propagation. The fracture origin is represented by flaws, impurities, or nonhomogeneous areas, from which the fracture starts to propagate.[47]

SEM micrographs of the representative specimens for each group are presented in Figure 3. For the statically loaded specimens, typical fracture patterns of a brittle failure, such as hackle lines and evident fracture origin, were observed (Figure 3A,C,E). The cyclically loaded specimens exhibited a smoother and more even appearance (Figure 3B,D), except for the cyclically loaded specimen in the 3D
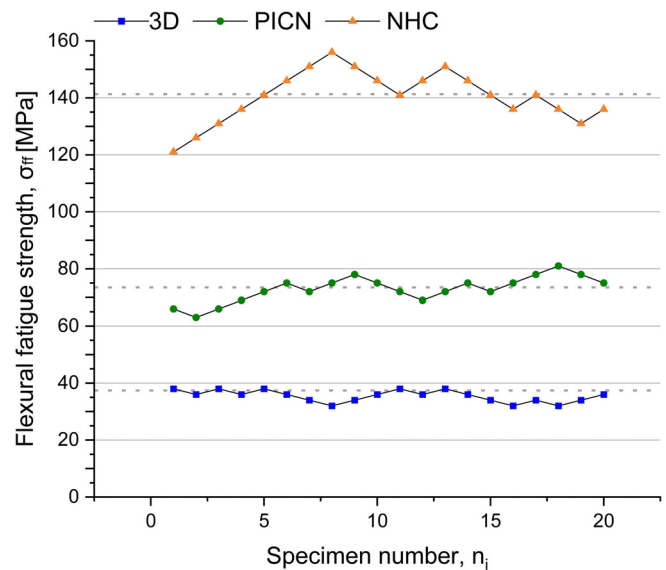

FIGURE 2 Biaxial flexural fatigue strength (σ_{ff}) for all three groups according to the staircase method. Dashed lines represent calculated σ_{ff} for each group. NHC, nanohybrid composite resin; PICN, polymer-infiltrated ceramic network; 3D, 3D-printed composite resin.

group, which failed after a smaller number of cycles (1542 cycles) (Figure 3F). In the majority of cases, the fractures originated from near-surface flaws, such as microcracks, pits, inclusions or nonhomogeneous areas.

In the cyclically loaded NHC specimen, crack propagation within the matrix and along the particle/matrix interface was observed (Figure 4A). In the cyclically loaded specimen in the 3D group, the crack propagated mainly through the polymer matrix (Figure 4B). At the fracture origin, nonhomogeneous areas where filler particles were not embedded in the polymer matrix, were observed. (Figure 4B). A surface inspection of the nonfractured, cyclically loaded specimens in the 3D group showed surface irregularities and microcracks (Figure 5A). Nonhomogeneous areas were also observed at the surface (Figure 5B).

4 | DISCUSSION

Based on the findings of this in vitro study, lower initial and fatigue biaxial flexural strengths were observed for the investigated 3D-printed composite resin. In addition, the fatigue susceptibility differed among the tested materials, with the highest strength degradation exhibited by the 3D-printed composite resin. Therefore, the first research hypothesis was accepted. Furthermore, differences in the fracture patterns among the differently manufactured composite resins were observed, where the fracture origin of the 3D-printed composite resin was associated with the flaws introduced during the 3D-printing procedure, accepting the second research hypothesis.

The experimental geometry for the biaxial strength testing was prepared following the established methodology,[37] based on the
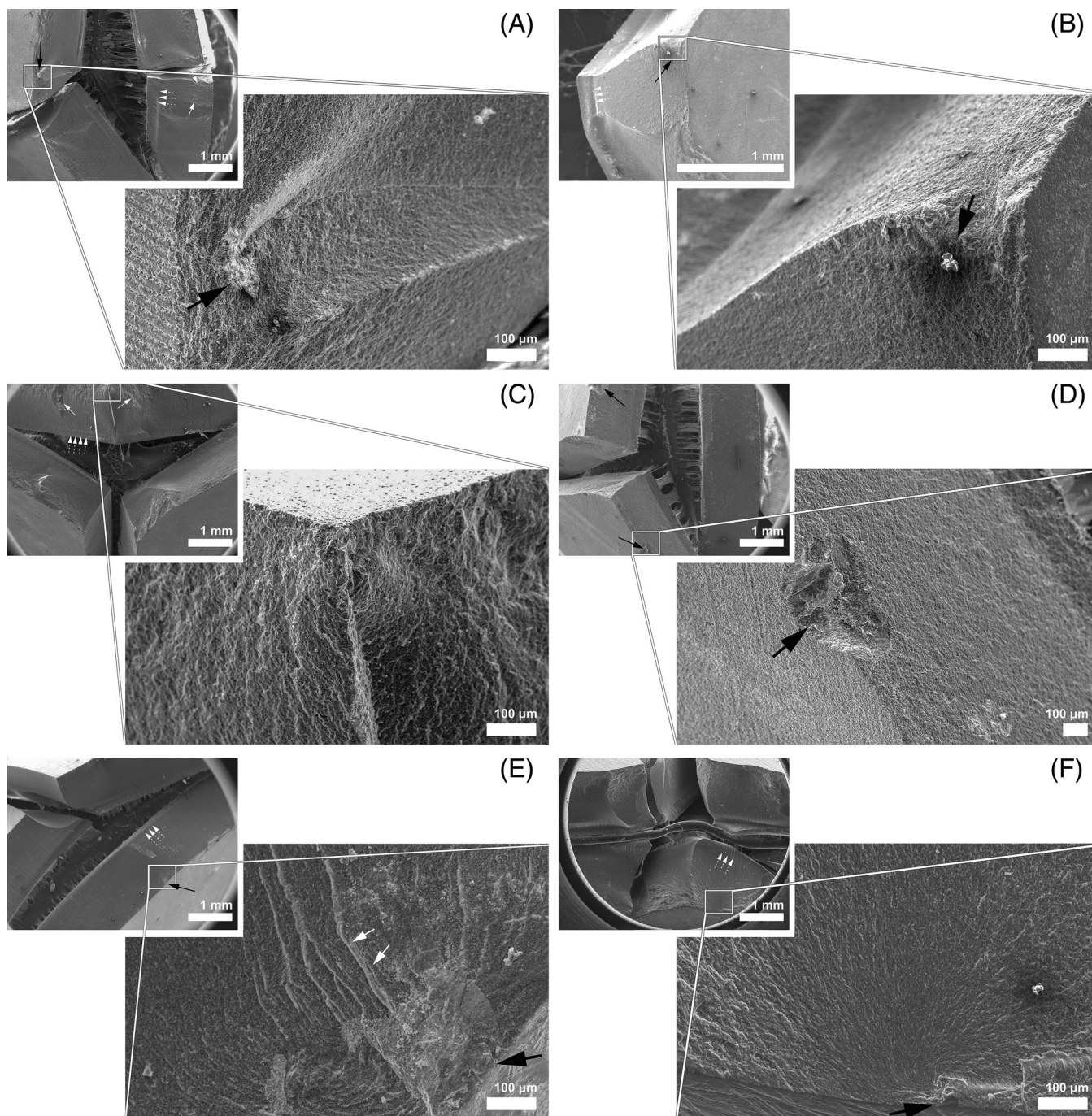
FIGURE 3 Scanning electron micrographs at low magnification (original magnification ×20) (figure inset) and higher magnification (original magnification ×200) of representative fractured specimens for each group that failed during static loading and cyclic loading. (A) NHC group statically loaded and (B) cyclically loaded specimens; (C) PICN group statically loaded and (D) cyclically loaded; (E) 3D group statically loaded and (F) cyclically loaded specimens. Black arrows indicate the fracture origin from which the crack started to propagate, white lines indicate hackles giving the direction of crack propagation, and dotted white lines indicate compressive curls that show the compression side of the specimen. NHC, nanohybrid composite resin; PICN, polymer-infiltrated ceramic network; 3D, 3D-printed composite resin.

international standard ISO 6872.[38] The disc thickness was slightly higher to ensure minimal deflection of the elastic specimens, which is the primary condition for obtaining valid strength-evaluation data.[48] Unlike the 3-point flexural test, the biaxial flexural tests induce a smaller stress zone at the center of the specimens. This approach lowers the stresses in the defective volume and removes the influence of

cracks at the specimens' edges, thus improving the reliability of the data.[45,49] In addition, an established storage protocol for testing composite resin[31,41] that includes 14 days of water immersion was employed to ensure adequate water sorption and facilitate the minimum hydrolytic degradation of the specimens, relating to the humid conditions of the oral environment.[42]

FIGURE 4 Scanning electron micrographs of crack propagation in representative cyclically loaded specimens. (A) Low-magnification (original magnification ×200) of the NHC specimen (upper micrograph). High-magnification (original magnification ×5000) of crack propagation through matrix/particle interface (left- and right-side micrographs; *white arrow*); (B) low-magnification (original magnification ×250) of the 3D specimen (upper micrograph). High-magnification (original magnification ×2000) of crack propagation through matrix interface (left side micrograph; *white arrow*); high-magnification (original magnification ×5000) of nonhomogeneous area (right side micrograph) with densely packed filler particles not embedded in the resin matrix (*black arrow*). NHC, nanohybrid composite resin; 3D, 3D-printed composite resin.
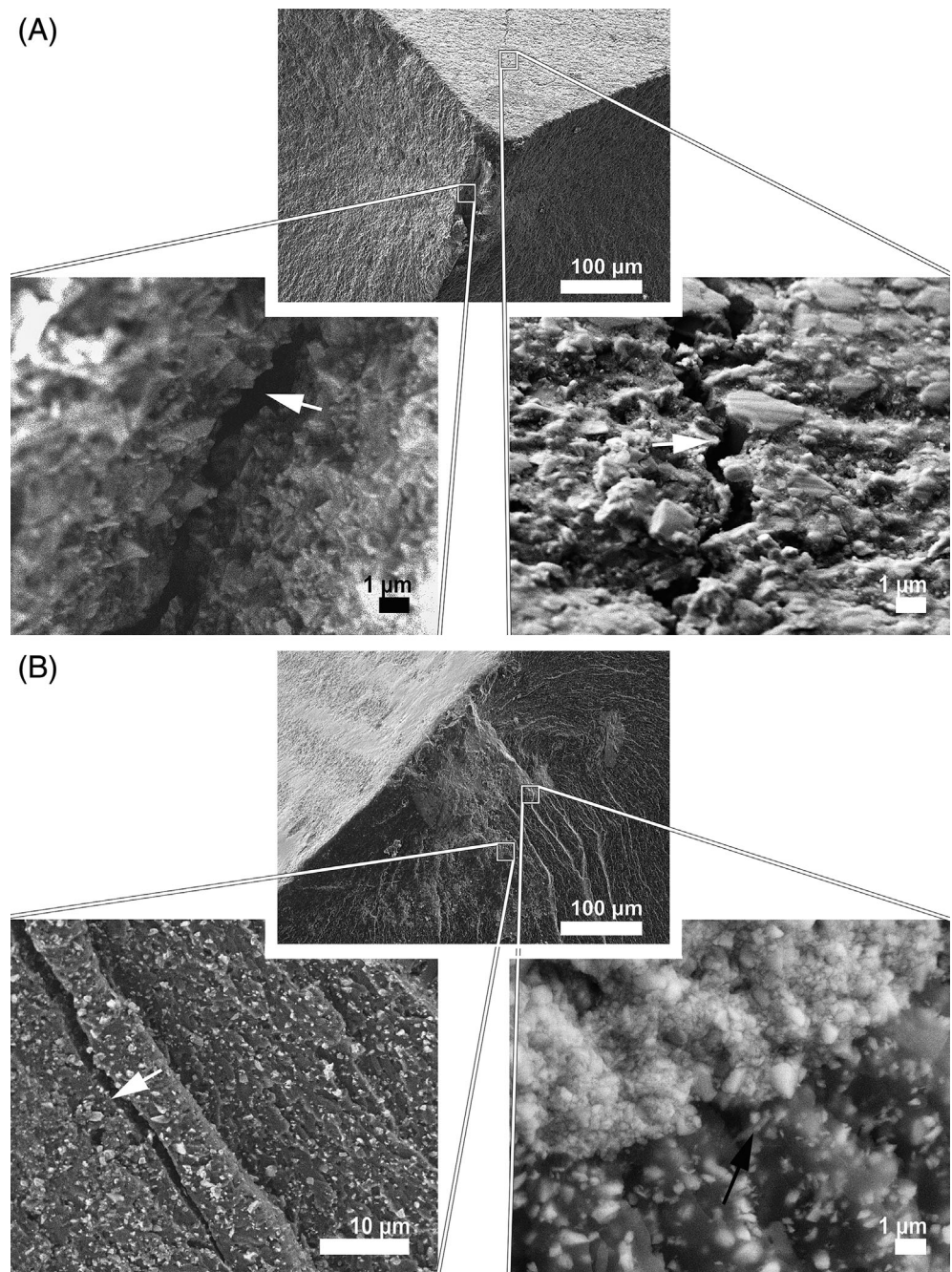
The initial biaxial flexural strength and material reliability, assessed by the Weibull analysis, varied significantly among the groups.[50] Different flaw populations among the tested groups probably resulted from the different manufacturing technologies and the microstructurally different materials. First, the investigated 3D-printed composite resin consists of a significantly smaller amount of inorganic filler (30–50 wt%), which has been shown to correlate linearly with the flexural strength,[51] explaining the inferior initial strength of the 3D group compared to the other two groups with larger amounts of filler (86 wt%) (Table 2). In addition, the lower reliability for the 3D-printed composite resin was indicated by a significantly lower Weibull modulus (m) (Figure 1). A typical brittle fracture pattern of the statically loaded specimens was observed with the SEM (Figure 3), probably a consequence of exceeding the elastic limit of the tested materials.

The initial biaxial flexural strengths calculated in our study are consistent with previous studies, wherein comparable[12,15,22,52] or slightly lower flexural strength values[14,15,24] were reported for the 3D-printed resins and composite resins. In contrast, some studies reported higher strength values than those in the present study.[11,13,16,17] Among these, two studies evaluated 3D-printed composite resins with an amount of filler similar to the 3D-printed material tested here,[11,18] while others either studied 3D-printed resins containing no filler[13] or did not report on the material's microstructure.[16,17] Such varying results could be
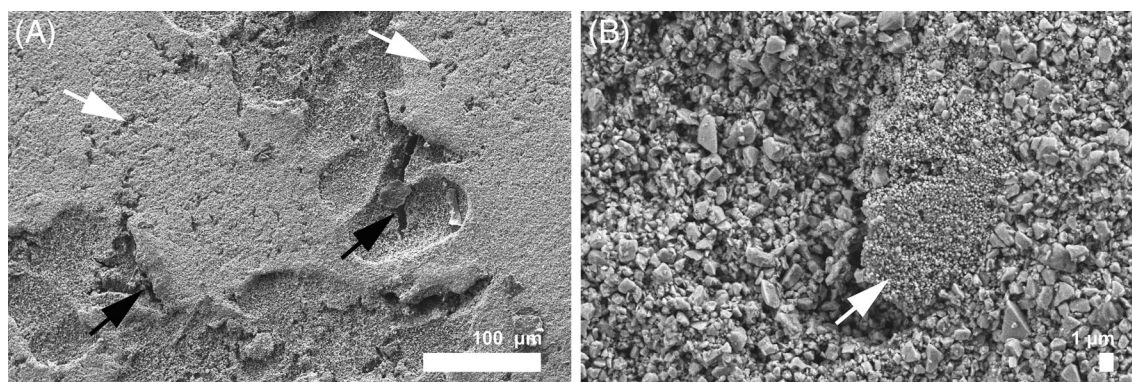
FIGURE 5 Scanning electron micrographs of nonfractured, cyclically loaded 3D-printed composite resin specimen. (A) Surface exhibiting small flaws (*white arrow*) and microcracks (*black arrow*) (original magnification ×250); (B) nonhomogeneous area in the surface (*white arrow*) (original magnification ×3000).

attributed to the differences in the experimental set-ups for measuring the flexural strength, the types of 3D-printing materials tested, and the printing strategies employed. In addition, the more extended water storage in our study, which promotes hydrolysis, could potentially have led to the lower strengths of the investigated 3D-printed composite resin.

Material processing played an important role in the inclusion of surface flaws observed in the investigated 3D-printed composite resin (Figure 5), which is in line with previous fractographic analyses.[14,16,18] It has been shown that a larger amount of filler might impair the resin's flow during the building platform's movements of the printer, increasing the risk of incorporating air voids and impairing the mechanical properties.[15] In contrast to these findings, no voids were observed in the investigated 3D-printed composite resin under the SEM. However, areas of nonhomogenous microstructure were identified as the fracture origins (Figures 4B and 5B), which probably arose from the inconsistent mixing of the composite resin's constituents. As such, the mixing procedure for the constituents of the investigated 3D-printed composite resin should be optimized to provide a more homogeneous distribution of the individual components, thus, ensuring optimal mechanical properties.[23,53]

The specimens in our study were printed vertically onto the platform, with the resulting layers perpendicular to the applied force since each printed layer acts as an impediment to fracture.[18] The layer thickness of 50 μm was adopted according to the manufacturer's instructions, whereas increasing the thickness to 100 μm could improve the mechanical properties by reducing the risk of printing errors and the inclusion of voids.[18,54] However, a trade-off for the better mechanical properties resulting from the described printing strategy might be a reduced precision and restoration fit, thereby impeding clinical use.

A phenomenological approach to calculating the fatigue strength and comparing the fatigue susceptibility, reflected in the relative strength degradation after a predefined cyclic loading, was used in our study. The NHC group exhibited the highest biaxial flexural fatigue strength, followed by the PICN group (Table 2, Figure 2). The lowest fatigue susceptibility exhibited by the NHC group is in contrast to previous findings that smaller filler-size composite resins possess lower stress-intensity thresholds and lower fatigue strengths.[55,56] Conversely, the resin matrix and its adhesion to filler particles represent a component more prone to slow crack propagation during fatigue.[57,58] Therefore, an almost 15% higher relative strength degradation in the 3D group probably resulted from a significantly larger amount of resin phase (Table 2, Figure 2), prone to creep deformation, water sorption, and hydrolysis.[57]

The cyclically loaded specimens exhibited two types of fractures. In the NHC and PICN specimens (Figure 3B,D), a smoother fracture surface might have resulted from subcritical crack growth, plastic deformation, or viscoelastic creep,[59,60] while the brittle fracture pattern in the 3D specimens (Figure 3F) might have corresponded to the smaller number of cycles until failure. Furthermore, the observed crack propagation in the matrix for the representative cyclically loaded 3D specimen under the SEM (Figure 4B) accords with the fatigue testing, confirming that the large matrix volume contributes to inferior fatigue strength.[23,53] In addition, the small surface cracks observed in the nonfractured, cyclically loaded 3D-printed composite resin specimen (Figure 5A) might have been introduced by the repeated contact stress during cyclic loading. These surface or subsurface microcracks can lead to fatigue wear or can gradually propagate, eventually resulting in failure, additionally explaining the lower biaxial flexural fatigue strength of the 3D-printed composite resin.[56,61]

Only a few studies investigated the fatigue behavior of 3D-printed composite resins, all employing cyclic loading before static testing.[20,26-28] In addition, none of these studies carried out a fractographic analysis to determine the fracture origins and patterns necessary to understand the shortcomings of an investigated material and its manufacture. Furthermore, only one study evaluated the flexural fatigue strength and susceptibility with a 3-point bending test, reporting a relatively small decrease in the flexural strength of approximately 3%–7% of the initial strength.[20] However, no comparison of the tested 3D-printed materials to the well-established milled composite resins was made. In addition, the almost insignificant strength degradation in this study can be related to cyclically loading the specimen with a loading force that was insufficient to

achieve the crack-propagation threshold, not creating any damage accumulation.[25,62] Therefore, a different methodology was used in our study, which is more effective in achieving the stress intensity necessary for crack propagation since the cyclic loads for each tested material were individually determined from the measured initial strength.[25]

Other studies evaluated the fatigue behavior of the 3D-printed composite resin using more complex experimental geometry specimens, which is difficult to directly compare with our results. Nevertheless, similarities with our study, in terms of the inferior fatigue behavior of the investigated 3D-printed composite resin, can be seen in studies where lower survival rates,[26] fracture loads,[27] and higher strength degradations[26] of the 3-unit FDPs fabricated from 3D-printed composite resins compared to the milled composite resins were reported. These similar findings could be explained by the bending moment over the biaxially loaded disc specimen, tested in our study, and the length of the 3-unit FDP, generating high tensile stresses in both experimental geometries.[16,63] In contrast, for 3D-printed composite resin crowns[28] and inlays,[9] a more encouraging performance was reported after the cyclic loading, however, still exhibiting lower fracture loads than the milled material.[28] This can be attributed to the different experimental geometry, where the crown or inlay is uniformly supported and bonded to the abutment tooth, offering a more favorable stress distribution.[64] However, since the initial fracture loads were not measured, no information about the strength degradation and the actual fatigue susceptibility of the 3D-printed composite resin could be derived.[28]

A rough estimation of the clinical behavior of the 3D-printed composite resin can be drawn from the present in vitro results.[29] A comparison of the distribution of the critical flaws, and especially the biaxial flexural fatigue strength, with the clinically validated composite resins in the groups NHC and PICN, indicate that the investigated 3D-printed composite resin might perform clinically less well and less reliably. Therefore, the clinical indications of the investigated 3D-printed composite resin, although proposed for definitive restorations, should be limited to long-term provisional restorations. The exception would be intracoronal restorations, such as inlays or small onlays, where flowable composite resins with similar mechanical properties were previously shown to be clinically acceptable.[65]

This study presents a more fundamental approach to investigating the fatigue behavior of a novel 3D-printed composite resin complemented by a detailed fractographic analysis, thereby deepening our knowledge of the fatigue-fracture patterns and possible fracture origins.[31,41] Such studies are essential to improve the material microstructure and manufacturing processes, yet they are currently absent. The main limitation of our study was that the staircase approach, although providing accurate estimations of the mean biaxial flexural fatigue strength, gives only a limited insight into the extended lifetime of the specimen.[25] In addition, despite testing a novel 3D-printed composite resin for definitive restorations, comparing it with at least one or more 3D-printed composite resins currently available on the market, would provide valuable information.

5 | CONCLUSIONS

Within the limitations of the present study, the following conclusions can be drawn:

1. The investigated 3D-printed composite resin exhibited a lower initial biaxial flexural strength and reliability compared to the tested milled composite resins.
2. The investigated 3D-printed composite resin exhibited a lower biaxial flexural fatigue strength compared to the tested milled composite resins, with a 9%–15% higher relative strength degradation.
3. For the investigated 3D-printed composite resin, areas of nonhomogeneous microstructure served as potential fracture origins.

CONFLICT OF INTEREST STATEMENT
The authors declare no conflicts of interest.

DATA AVAILABILITY STATEMENT
The data that support the findings of this study are available from the corresponding author [P.J.], upon reasonable request.

ORCID
Tine Malgaj https://orcid.org/0000-0002-0296-9814

REFERENCES
1. Schlichting LH, Resende TH, Reis KR, Raybolt Dos Santos A, Correa IC, Magne P. Ultrathin CAD-CAM glass-ceramic and composite resin occlusal veneers for the treatment of severe dental erosion: an up to 3-year randomized clinical trial. *J Prosthet Dent*. 2022;128(2):158.e1–158.e12.
2. Edelhoff D, Erdelt KJ, Stawarczyk B, Liebermann A. Pressable lithium disilicate ceramic versus CAD/CAM resin composite restorations in patients with moderate to severe tooth wear: clinical observations up to 13 years. *J Esthet Restor Dent*. 2023;35(1):116-128.
3. Kunzelmann KH, Jelen B, Mehl A, Hickel R. Wear evaluation of MZ100 compared to ceramic CAD/CAM materials. *Int J Comput Dent*. 2001;4(3):171-184.
4. Magne P, Perakis N, Belser UC, Krejci I. Stress distribution of inlay-anchored adhesive fixed partial dentures: a finite element analysis of the influence of restorative materials and abutment preparation design. *J Prosthet Dent*. 2002;87(5):516-527.
5. Magne P, Schlichting LH, Maia HP, Baratieri LN. In vitro fatigue resistance of CAD/CAM composite resin and ceramic posterior occlusal veneers. *J Prosthet Dent*. 2010;104(3):149-157.
6. Magne P, Paranhos MP, Schlichting LH. Influence of material selection on the risk of inlay fracture during pre-cementation functional occlusal tapping. *Dent Mater*. 2011;27(2):109-113.

7. Baba NZ, Goodacre BJ, Goodacre CJ, Muller F, Wagner S. CAD/CAM complete denture systems and physical properties: a review of the literature. *J Prosthodont*. 2021;30(S2):113-124.

8. Alghazzawi TF. Advancements in CAD/CAM technology: options for practical implementation. *J Prosthodont Res*. 2016;60(2):72-84.

9. Daher R, Ardu S, di Bella E, Krejci I, Duc O. Efficiency of 3D-printed composite resin restorations compared with subtractive materials: evaluation of fatigue behavior, cost, and time of production. *J Prosthet Dent*. 2022.

10. Ligon SC, Liska R, Stampfl J, Gurr M, Mulhaupt R. Polymers for 3D printing and customized additive manufacturing. *Chem Rev*. 2017; 117(15):10212-10290.

11. Grzebieluch W, Kowalewski P, Grygier D, Rutkowska-Gorczyca M, Kozakiewicz M, Jurczyszyn K. Printable and machinable dental restorative composites for CAD/CAM application-comparison of mechanical properties, fractographic, texture and fractal dimension analysis. *Materials (Basel)*. 2021;14(17):4919.

12. Lin CH, Lin YM, Lai YL, Lee SY. Mechanical properties, accuracy, and cytotoxicity of UV-polymerized 3D printing resins composed of Bis-EMA, UDMA, and TEGDMA. *J Prosthet Dent*. 2020;123(2):349-354.

13. Bayarsaikhan E, Gu H, Hwangbo NK, et al. Influence of different post-curing parameters on mechanical properties and biocompatibility of 3D printed crown and bridge resin for temporary restorations. *J Mech Behav Biomed Mater*. 2022;128:105127.

14. Bergamo ETP, Campos TMB, Piza MMT, et al. Temporary materials used in prosthodontics: the effect of composition, fabrication mode, and aging on mechanical properties. *J Mech Behav Biomed Mater*. 2022;133:105333.

15. de Castro EF, Nima G, Rueggeberg FA, Giannini M. Effect of build orientation in accuracy, flexural modulus, flexural strength, and microhardness of 3D-printed resins for provisional restorations. *J Mech Behav Biomed Mater*. 2022;136:105479.

16. Atria PJ, Bordin D, Marti F, et al. 3D-printed resins for provisional dental restorations: comparison of mechanical and biological properties. *J Esthet Restor Dent*. 2022;34(5):804-815.

17. Taşın S, Ismatullaev A. Comparative evaluation of the effect of thermocycling on the mechanical properties of conventionally polymerized, CAD-CAM milled, and 3D-printed interim materials. *J Prosthet Dent*. 2022;127(1):173.e171–173.e178.

18. Kessler A, Hickel R, Ilie N. In vitro investigation of the influence of printing direction on the flexural strength, flexural modulus and fractographic analysis of 3D-printed temporary materials. *Dent Mater J*. 2021;40(3):641-649.

19. Ribeiro AKC, de Freitas R, de Carvalho IHG, et al. Flexural strength, surface roughness, micro-CT analysis, and microbiological adhesion of a 3D-printed temporary crown material. *Clin Oral Investig*. 2023;27(5):2207-2220.

20. Scherer MD, Barmak AB, Özcan M, Revilla-León M. Influence of post-polymerization methods and artificial aging procedures on the fracture resistance and flexural strength of a vat-polymerized interim dental material. *J Prosthet Dent*. 2022;128(5):1085-1093.

21. Al-Haj Husain N, Feilzer AJ, Kleverlaan CJ, Abou-Ayash S, Ozcan M. Effect of hydrothermal aging on the microhardness of high- and low-viscosity conventional and additively manufactured polymers. *J Prosthet Dent*. 2022;128(4):822.e821–822.e829.

22. Soto-Montero J, de Castro EF, Romano BC, Nima G, Shimokawa CAK, Giannini M. Color alterations, flexural strength, and microhardness of 3D printed resins for fixed provisional restoration using different post-curing times. *Dent Mater*. 2022;38(8):1271-1282.

23. Kessler A, Reymus M, Hickel R, Kunzelmann KH. Three-body wear of 3D printed temporary materials. *Dent Mater*. 2019;35(12):1805-1812.

24. Scotti CK, Velo M, Rizzante FAP, Nascimento TRL, Mondelli RFL, Bombonatti JFS. Physical and surface properties of a 3D-printed composite resin for a digital workflow. *J Prosthet Dent*. 2020;124(5):614.e611–614.e615.

25. Kelly JR, Cesar PF, Scherrer SS, et al. ADM guidance-ceramics: fatigue principles and testing. *Dent Mater*. 2017;33(11):1192-1204.

26. Nold J, Wesemann C, Rieg L, et al. Does printing orientation matter? In-vitro fracture strength of temporary fixed dental prostheses after a 1-year simulation in the artificial mouth. *Materials (Basel)*. 2021;14(2):259.

27. Zimmermann M, Ender A, Attin T, Mehl A. Fracture load of three-unit full-contour fixed dental prostheses fabricated with subtractive and additive CAD/CAM technology. *Clin Oral Investig*. 2020;24(2):1035-1042.

28. Rosentritt M, Rauch A, Hahnel S, Schmidt M. In-vitro performance of subtractively and additively manufactured resin-based molar crowns. *J Mech Behav Biomed Mater*. 2023;141:105806.

29. Garcia-Godoy F, Frankenberger R, Lohbauer U, Feilzer AJ, Kramer N. Fatigue behavior of dental resin composites: flexural fatigue in vitro versus 6 years in vivo. *J Biomed Mater Res B Appl Biomater*. 2012; 100(4):903-910.

30. Wendler M, Belli R, Valladares D, Petschelt A, Lohbauer U. Chairside CAD/CAM materials. Part 3: cyclic fatigue parameters and lifetime predictions. *Dent Mater*. 2018;34(6):910-921.

31. Belli R, Petschelt A, Lohbauer U. Are linear elastic material properties relevant predictors of the cyclic fatigue resistance of dental resin composites? *Dent Mater*. 2014;30(4):381-391.

32. Eldafrawy M, Nguyen JF, Mainjot AK, Sadoun MJ. A functionally graded PICN material for biomimetic CAD-CAM blocks. *J Dent Res*. 2018;97(12):1324-1330.

33. Spitznagel FA, Scholz KJ, Strub JR, Vach K, Gierthmuehlen PC. Polymer-infiltrated ceramic CAD/CAM inlays and partial coverage restorations: 3-year results of a prospective clinical study over 5 years. *Clin Oral Investig*. 2018;22(5):1973-1983.

34. Dukic W, Dukic OL, Milardovic S, Delija B. Clinical evaluation of indirect composite restorations at baseline and 36 months after placement. *Oper Dent*. 2010;35(2):156-164.

35. Cetin AR, Unlu N, Cobanoglu N. A five-year clinical evaluation of direct nanofilled and indirect composite resin restorations in posterior teeth. *Oper Dent*. 2013;38(2):E1-E11.

36. Oudkerk J, Eldafrawy M, Bekaert S, Grenade C, Vanheusden A, Mainjot A. The one-step no-prep approach for full-mouth rehabilitation of worn dentition using PICN CAD-CAM restorations: 2-yr results of a prospective clinical study. *J Dent*. 2020;92:103245.

37. Cotic J, Jevnikar P, Kocjan A. Ageing kinetics and strength of airborne-particle abraded 3Y-TZP ceramics. *Dent Mater*. 2017;33(7):847-856.

38. ISO 6872. *Dentistry – Dental Ceramics*. International Organization for Standards; 1999.

39. Della Bona A, Corazza PH, Zhang Y. Characterization of a polymer-infiltrated ceramic-network material. *Dent Mater*. 2014;30(5):564-569.

40. Papadogiannis DY, Lakes RS, Papadogiannis Y, Palaghias G, Helvatjoglu-Antoniades M. The effect of temperature on the viscoelastic properties of nano-hybrid composites. *Dent Mater*. 2008;24(2):257-266.

41. Belli R, Geinzer E, Muschweck A, Petschelt A, Lohbauer U. Mechanical fatigue degradation of ceramics versus resin composites for dental restorations. *Dent Mater*. 2014;30(4):424-432.

42. Lohbauer U, Belli R. The mechanical performance of a novel self-adhesive restorative material. *J Adhes Dent*. 2020;22(1):47-58.

43. Draughn RA. Compressive fatigue limits of composite restorative materials. *J Dent Res*. 1979;58(3):1093-1096.

44. Dixon WJ, Mood AM. A method for obtaining and analyzing sensitivity data. *J Am Stat Assoc*. 1948;43(241):109-126.

45. Ilie N, Hilton TJ, Heintze SD, et al. Academy of dental materials guidance-resin composites: Part I-mechanical properties. *Dent Mater*. 2017;33(8):880-894.

46. EN 843-5. Advanced technical ceramics – mechanical properties of monolithic ceramics at room temperature, Part 5 Stat. Anal. 2006.

47. Scherrer SS, Lohbauer U, Della Bona A, et al. ADM guidance-ceramics: guidance to the use of fractography in failure analysis of brittle materials. *Dent Mater*. 2017;33(6):599-620.

48. Morell R. *Biaxial Flexural Strength Testing of Ceramic Materials: A National Measurement Good Practice Guide No. 12*. National Physical Laboratory; 2007.

49. Palin WM, Fleming GJ, Marquis PM. The reliability of standardized flexure strength testing procedures for a light-activated resin-based composite. *Dent Mater*. 2005;21(10):911-919.

50. McCabe JF, Carrick TE. A statistical approach to the mechanical testing of dental materials. *Dent Mater*. 1986;2(4):139-142.

51. Kim K-H, Ong JL, Okuno O. The effect of filler loading and morphology on the mechanical properties of contemporary composites. *J Prosthet Dent*. 2002;87(6):642-649.

52. Aati S, Chauhan A, Shrestha B, Rajan SM, Aati H, Fawzy A. Development of 3D printed dental resin nanocomposite with graphene nanoplatelets enhanced mechanical properties and induced drug-free antimicrobial activity. *Dent Mater*. 2022;38(12):1921-1933.

53. Prause E, Hey J, Beuer F, Schmidt F. Wear resistance of 3D-printed materials: a systematic review. *Dent Rev*. 2022;2(2):100051.

54. Tahayeri A, Morgan M, Fugolin AP, et al. 3D printed versus conventionally cured provisional crown and bridge dental materials. *Dent Mater*. 2018;34(2):192-200.

55. Shah MB, Ferracane JL, Kruzic JJ. Mechanistic aspects of fatigue crack growth behavior in resin based dental restorative composites. *Dent Mater*. 2009;25(7):909-916.

56. Turssi CP, Ferracane JL, Ferracane LL. Wear and fatigue behavior of nano-structured dental resin composites. *J Biomed Mater Res B Appl Biomater*. 2006;78(1):196-203.

57. Ferracane JL. Hygroscopic and hydrolytic effects in dental polymer networks. *Dent Mater*. 2006;22(3):211-222.

58. Lohbauer U, Belli R, Ferracane JL. Factors involved in mechanical fatigue degradation of dental resin composites. *J Dent Res*. 2013;92(7):584-591.

59. Lohbauer U, von der Horst T, Frankenberger R, Kramer N, Petschelt A. Flexural fatigue behavior of resin composite dental restoratives. *Dent Mater*. 2003;19(5):435-440.

60. Ornaghi BP, Meier MM, Lohbauer U, Braga RR. Fracture toughness and cyclic fatigue resistance of resin composites with different filler size distributions. *Dent Mater*. 2014;30(7):742-751.

61. Kruzic JJ, Arsecularatne JA, Tanaka CB, Hoffman MJ, Cesar PF. Recent advances in understanding the fatigue and wear behavior of dental composites and ceramics. *J Mech Behav Biomed Mater*. 2018;88:504-533.

62. Heintze SD, Eser A, Monreal D, Rousson V. Using a chewing simulator for fatigue testing of metal ceramic crowns. *J Mech Behav Biomed Mater*. 2017;65:770-780.

63. Bataineh K, Al Janaideh M, Abu-Naba'a LA. Fatigue resistance of 3-unit CAD-CAM ceramic fixed partial dentures: an FEA study. *J Prosthodont*. 2022;31(9):806-814.

64. Kelly JR. Clinically relevant approach to failure testing of all-ceramic restorations. *J Prosthet Dent*. 1999;81(6):652-661.

65. Torres CRG, Rêgo HMC, Perote LCCC, et al. A split-mouth randomized clinical trial of conventional and heavy flowable composites in class II restorations. *J Dent*. 2014;42(7):793-799.